

Cyclotron Resonance in a Pure Electron Plasma Column

Roy W. Gould and Michael A. LaPointe

Department of Applied Physics, California Institute of Technology, Pasadena, California 91125

(Received 16 September 1991)

We demonstrate experimentally the effects of plasma rotation and particle thermal velocities on cyclotron resonance in a long cylindrical pure electron plasma column of low density ($\omega_p^2 \ll \omega_c^2$). A single $m=1$ mode ($e^{im\theta - i\omega t}$) is found whose frequency ω is down-shifted from $\omega_c = eB/m_e$ by an amount equal to the low-frequency diocotron mode frequency ($\langle \omega_p^2 \rangle / 2\omega_c$). For $m=2, 3, 4, \dots$ sets of modes are found which are Doppler shifted upward from ω_c . We explain these as radially trapped and azimuthally propagating Bernstein modes.

PACS numbers: 52.25.Wz, 52.35.Fp

There has been considerable interest in non-neutral plasmas in the past decade. Experimental work has tended to focus on low-frequency phenomena [1] such as eigenmodes and instabilities [2], cooling [3], approach to thermal equilibrium [4], and transport [5]. Little attention has been given to high-frequency phenomena, e.g., cyclotron resonance, of obvious importance for beam devices such as gyrotrons and free-electron lasers. Although cyclotron resonance is used for mass measurements [6], the densities are generally low enough that plasma effects are unimportant. In this paper we report the observation of plasma effects on cyclotron resonance in pure electron plasmas, including Doppler shift due to plasma rotation and trapped Bernstein modes due to plasma thermal velocities.

We have explored experimentally the response of a cylindrical pure electron plasma column to weak rf electric fields near the electron cyclotron frequency $\omega_c = eB/m_e$, and the various plasma effects which arise. Because of the unneutralized charge, there is a radial electric field which causes an $\mathbf{E} \times \mathbf{B}$ plasma rotation. In laboratory plasmas generally, the electron density n_0 and thus the rotational angular velocity of the plasma, ω_0 , depend upon radius, in contrast with the rigid-rotor equilibrium state where $\omega_0 = \text{const}$, often studied theoretically [7-9]. $\omega_0(r)$ is determined [10] from the plasma density by $(1/r)(d/dr)[r^2\omega_0(r)] = \omega_p^2(r)/\omega_c$, where $\omega_p = [n_0(r)e^2/\epsilon_0 m_e]^{1/2}$ is the plasma frequency. The density parameter $\omega_p^2/\omega_c^2 \approx 0.01$ so that plasma effects, including the Doppler shift due to plasma rotation, introduce correspondingly small shifts from the cyclotron frequency. Our investigation emphasizes this limited range.

The experiment shown schematically in Fig. 1 is a segmented cylindrical electrode structure designed so that various multipolar rf fields ($e^{im\theta - i\omega t}$) can be applied. The cylinder radius is 2.5 cm and the plasma length is about 40 cm. Since $B \approx 50$ G, $f_c \approx 140$ MHz. The device is operated in the usual repetitive inject-trap-dump cycle [10]. During the trap phase, the plasma density decays as in other such devices by mechanisms not fully understood [5]. We exploit the density decay to provide a density scan on each cycle. The decay time is typically 80

msec, and the trapping time 200 msec. Thus the density decays by a factor of 10-12.

Figures 1(b)-1(e) show some possible phasings of the applied rf potentials. Ideally, configurations (c) and (d) of the octupole sections excite $m = \pm 1, \pm 3, \pm 5, \dots$ and $m = \pm 2, \pm 6, \dots$ modes, respectively. Configuration (e) generates an azimuthally traveling wave with a rotating applied electric field. The axial segmentation of the cylinder also gives rise to a k_z spectrum, but the modes we describe below are those with $k_z \approx 0$. Configuration (b) is used to excite the low-frequency $m=1$ diocotron mode [2,10] with one dipole section and to receive it on the other dipole section. The frequency of the $m=1$ diocotron mode [11] is $\omega_d = \langle \omega_p^2 \rangle / 2\omega_c$, where $\langle \rangle$ indicates an average over the cylinder cross section. ω_d gives a measure of the average plasma density, as does the charge collected upon dump.

Figure 2 shows the transmission from one octupole section to the other during the plasma decay. The rf source is on continuously at the 1-3 mV level. The frequency is

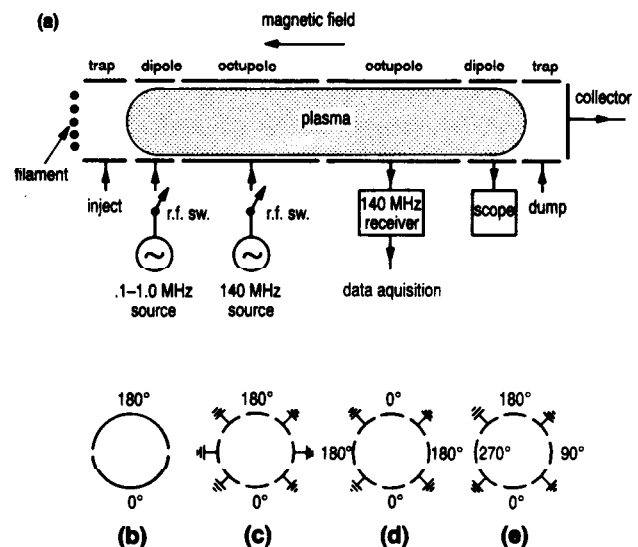


FIG. 1. (a) Schematic of cylindrical electrode structure and instrumentation. (b)-(e) Possible phasing of dipole and octupole sections.

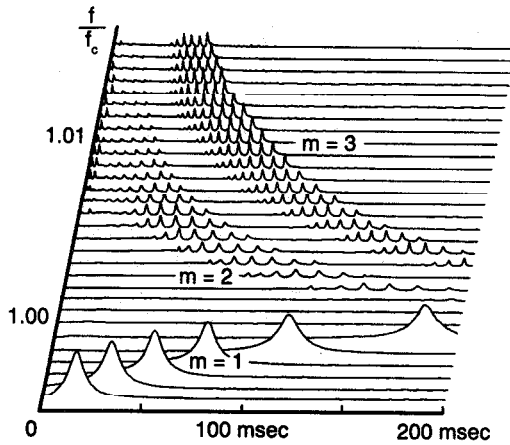


FIG. 2. Transmission vs time during plasma decay. The magnetic field is decremented on successive traces. For clarity every fifth trace is displayed. The $m=4$ resonances are too small to be seen in this display.

fixed (142.00 MHz) and on each trace the magnetic field is decremented by a small amount. Thus this figure represents a two-dimensional scan in density (across) and magnetic field (down). Identification of the m values shown has been made using various excitation configurations such as shown in Figs. 1(c)-1(e). We see that there is a single $m = +1$ resonance whose frequency lies slightly below the cyclotron frequency by an amount which decreases with decreasing density. We also see sets of discrete resonances which fall into bands, one band for each positive m value. These lie somewhat above the cyclotron frequency by amounts which decrease with decreasing density and with decreasing m .

We first discuss the frequency of the $m = +1$ cyclotron resonance and its dependence upon plasma density. This dependence has been determined by measuring the $m = +1$ frequency with an rf burst which is gated on for 200 μ sec just prior to dump and by also measuring the collected charge at dump. By repeating this for various trap phase durations, the $m = +1$ cyclotron resonance frequency can be mapped out as a function of collected charge. We find that this frequency is *down-shifted* from ω_c in proportion to collected charge and thus to average density. A second method for determining the average density is to measure ω_d , the frequency of the $m = 1$ diocotron mode using the dipole sections shown in Fig. 1. Using the gated source procedure we found that ω_d was proportional to collected charge as expected. In a variation of this technique, which eliminates the collected charge from the measurement, we gated one source on immediately after gating the other source off and thus determined both the $m = +1$ cyclotron frequency and ω_d at very nearly the same time, and thus under similar plasma conditions. This was done at various times during the plasma decay, i.e., at various densities. The pairs of frequencies are cross-plotted in Fig. 3(a). A least-squares fit to the experimental data is also shown. The intercept

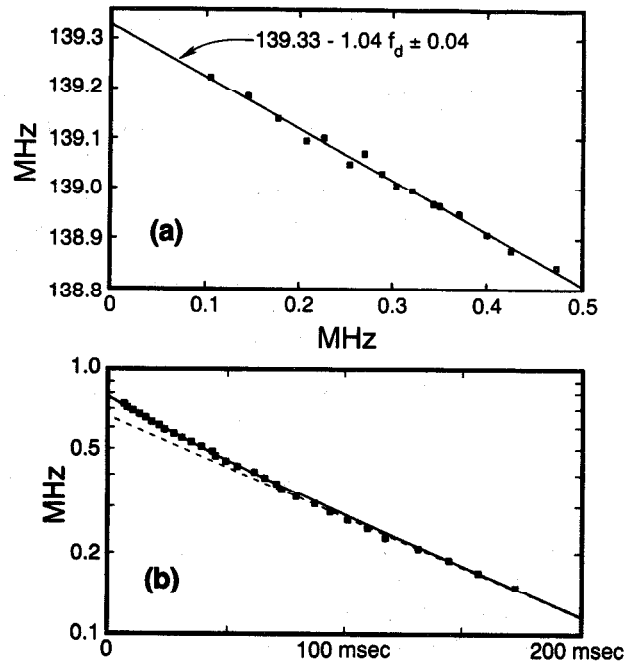


FIG. 3. (a) $m-1$ cyclotron resonance frequency vs $m-1$ diocotron frequency. (b) Decay of the $m=1$ cyclotron shift $\Delta\omega_1$ (mean density) vs time for the data of Fig. 2. Solid curve is a two-exponential fit.

of the curve is the single-particle cyclotron frequency and we find that the slope of the resulting data is -1.0 to within experimental error. Thus the *down-shift of the $m = +1$ cyclotron resonance is equal to the $m = 1$ diocotron frequency* and both are measures of the average density. One can trace this $m = 1$ result directly to the electric field $E_x = -(m/2e)\langle\omega_p^2\rangle\delta_x$ caused by the rearrangement of charges on the conducting wall when the column as a whole is displaced by a small amount δ_x . This electric field gives rise to a low-frequency drift of the column around the axis at frequency ω_d . It also affects the high-frequency motion of the column about the axis. Since the force from this electric field is antiparallel to the $\mathbf{v} \times \mathbf{B}$ force it also causes a slight *decrease*, equal to ω_d , in the frequency of this motion from ω_c .

Figure 3(b) shows the down-shift $\Delta\omega_1$ from the data of Fig. 2. The down-shift is well fitted by two exponentials, $\Delta\omega_1(t) = A_1 e^{-\gamma_1 t} + A_2 e^{-\gamma_2 t}$, and in the analysis of the data presented below we use this relationship for $\Delta\omega_1(t)$.

Data such as shown in Fig. 2 have been scanned to determine the time at which each resonance occurs and, using the $\Delta\omega_1(t)$ relationship, this time can be converted to average density, i.e., a value of $\Delta\omega_1$. Thus we are able to map out the dependence of *each* resonance upon average plasma density and magnetic field for a fixed frequency. Since the shift of a given resonance from the cyclotron frequency decreases with decreasing density, we introduce a normalized frequency shift, $(\omega - \omega_c)/\Delta\omega_1 \equiv \Omega$ which removes the density dependence. In Fig. 4 we plot the values of Ω for each resonance versus $\Delta\omega_1$. Points

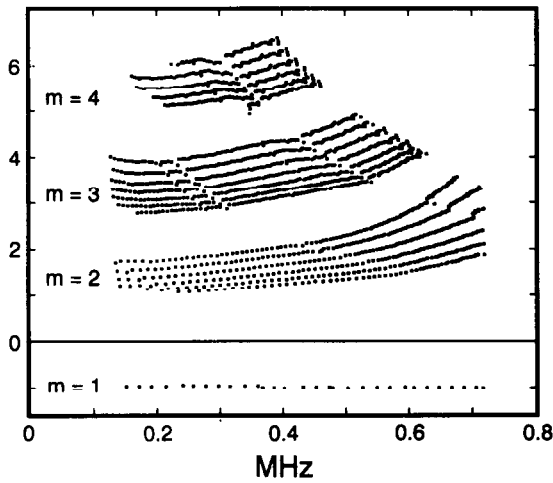


FIG. 4. Normalized frequency shifts, $(\omega - \omega_c)/\Delta\omega_1 = \Omega$, vs $\Delta f_1 = \Delta\omega_1/2\pi$ (mean density) from the data of Fig. 2.

representing the $m = +1$ resonance fall below the line at $\Omega \approx -1$, and points representing the $m = +2, +3, +4, \dots$ sets of resonances lie above in well defined bands. There is still a minor dependence upon average density ($\Delta\omega_1$), or time in the decay, and we think that this may result from evolution of the radial density profile as the plasma decays.

We now sketch our theoretical arguments to explain these results. For electrostatic waves propagating perpendicular to \mathbf{B} the plasma response can be characterized by the perpendicular dielectric function $K = 1 - \omega_p^2/(\omega'^2 - \omega_c^2)$, where $\omega' = \omega - m\omega_0$ is the Doppler shifted frequency at radius r in the rotating plasma and $\omega_c^2 = (\omega_c - 2\omega_0)(\omega_c - 2\omega_0 - r d\omega_0/dr)$ is the square of the single-particle gyration frequency at r [12,13]. Using the fact that ω_0/ω_c is small and keeping only first-order terms K can be rewritten as

$$K(r) = 1 - \frac{f(r)}{\lambda - mg(r) + g(r) + f(r)}, \quad (1)$$

where $f(r) = \omega_p^2(r)/\omega_p^2(0)$ and $g(r) = \omega_0(r)/\omega_0(0)$ are the normalized density and angular velocity functions and $\lambda = (\omega - \omega_c)/\omega_0(0)$ is the normalized frequency. Note that this normalization is to the central rotation frequency $\omega_0(0)$ of the plasma rather than to $\Delta\omega_1 (= \omega_d)$ which was used in presenting the experimental data. Thus the normalized experimental frequencies Ω differ from the normalized theoretical frequencies λ given below by a numerical factor. The term $mg(r)$ in the denominator of Eq. (1) is associated with the Doppler shift due to rotation and the terms $g(r) + f(r)$ are associated with a down-shift of the single-particle gyration frequency due to the centrifugal and Coriolis forces [12,13]. These three terms in the denominator would be absent in the corresponding result for a neutral plasma. The condition for a spatially localized hybrid resonance is given by $K(r) = 0$ where Eq. (1) is to be used. Continuum absorp-

tion bands are thus expected in the ranges

$$(m-1)g_{\min} \leq \lambda \leq (m-1)g_{\max}, \quad m = 1, 2, 3, \dots \quad (2)$$

Only applied fields with $m > 0$ are right circularly polarized and can excite cyclotron resonance. Assuming that $f(r) = 1 - (r/a)^2$, closely approximating a diffusion profile, $g(r) = 1 - 0.5(r/a)^2$, $g_{\min} = 0.5$, and $g_{\max} = 1.0$. For this particular profile, the central rotation frequency $\omega_0(0)$ is exactly a factor of 2 higher than the diocotron frequency ω_d and the shift $\Delta\omega_1$. Note that the $m = 1$ resonance is special; the continuum collapses to $\lambda = 0$. However, it can be shown [12] that there is a single discrete global mode with normalized frequency $\lambda = -\langle f(r) \rangle$. This down-shift arises from image charges in the wall as previously described.

When the finite, but small, temperature T of the plasma is taken into account, finite-Larmor-radius effects become important. Adjacent radii are coupled together and radially propagating Bernstein modes [14] result. We follow a procedure similar to that of Buchsbaum and Hasegawa [15] for Bernstein modes in a neutral plasma. To first order in T , Eq. (1) is modified to

$$K(r) = 1 - \frac{f(r)(1 - 0.5\rho^2 k^2)}{\lambda - mg(r) + g(r) + f(r)}, \quad (3)$$

where $\rho^2 = 2T/m\omega_c^2$ is the mean square Larmor radius and $k^2 = -\nabla^2$ is the square of the local wave number. Setting $K = 0$ gives a radial wave equation for radially trapped Bernstein modes

$$(1/r)d(rR)/dr - m^2 R/r^2 + \kappa^2(r)R = 0, \quad (4)$$

where $\kappa^2(r) = 2[(m-1)g(r) - \lambda]/\rho^2 f(r)$, κ is the local wave number, and R is proportional to the perturbed density [16]. This equation describes radially trapped eigenmodes in the frequency bands given by Eq. (2). For modes trapped near the axis, $f(r) \approx 1$. For the assumed profiles and $m > 1$, Eq. (4) is similar to the 2D harmonic oscillator equation and its eigenvalues are

$$\lambda_{lm} = (m-1) - \sqrt{m-1}(2l+m-1)\rho/a, \quad (5)$$

where $l = 1, 2, 3, \dots$ is the radial mode number. ρ/a is small in this experiment so Eq. (5) gives a series of closely spaced resonant frequencies, the uppermost of which lies just below the limiting values of $\lambda = 1, 2, 3, \dots$ for $m = 2, 3, 4, \dots$, respectively. The Doppler effect of rotation causes these modes to be *up-shifted* from the cyclotron frequency.

In comparing the experimental shifts Ω with the theoretical shifts λ , we must take into account the difference in normalization of Ω and λ . The Ω 's have been normalized to the average density whereas the λ 's have been normalized to the peak density. For the assumed profile, these differ by a factor of 2, so that $\Omega_{\text{theor}} = 2\lambda$. For the $m = +1$ resonance $\lambda = \langle f \rangle = -0.5$ so that in Fig. 4 the $m = 1$ shift should be -1 and the $m = +2, +3, +4$ shifts should lie below 2, 4, 6. In addi-

tion, the first few modes of each series, which are trapped near the axis, should have equal spacing. This is approximately what is observed. From a comparison of the observed mode spacings for each m with Eq. (5), an estimate of ρ/a is found to be 0.04 ± 0.01 . This implies $T \approx 2$ eV, consistent with that found in other experiments [1,10].

Our proposed explanation assumes Bernstein modes which are trapped in the core of the plasma and a diffusionlike density profile which extends to the conducting wall where the density vanishes. The general agreement of this model with the experiment is surprisingly good. However, we wish to point out that only two of its features are important: the ratio of central to mean density, $n_0(0)/\langle n_0(r) \rangle$, and the ratio of the rms electron Larmor radius to the "curvature" of the density profile on the axis, ρ/a . The lowest (small l) modes evanesce outside a critical radius which is close to the axis so that details of the density profile, including boundary conditions at or near the wall [14], are relatively unimportant. The relative independence of the results of Fig. 4 on density suggests that these ratios change only slightly during the plasma decay. Finally, we point out the differences with the Buchsbaum-Hasegawa modes in a neutral plasma column [15]. Our trapped modes depend critically on the rotational angular velocity profile, are near ω_c rather than $2\omega_c$, and have $m \geq 1$ rather than $m = 0$.

This work was supported by ONR Grant No. N00014-89-J-1264 and one of us (R.W.G.) gratefully acknowledges stimulating discussions with C. F. Driscoll, J. H. Malmberg, and T. M. O'Neil about non-neutral plas-

mas.

-
- [1] *Non-Neutral Plasma Physics*, edited by C. W. Roberson and C. F. Driscoll, AIP Conf. Proc. No. 175 (AIP, New York, 1988).
 - [2] K. S. Fine, C. F. Driscoll, and J. H. Malmberg, *Phys. Rev. Lett.* **63**, 2975 (1989).
 - [3] D. J. Heinzen, J. J. Bollinger, F. L. Moore, Wayne M. Itano, and D. J. Wineland, *Phys. Rev. Lett.* **66**, 2080 (1991).
 - [4] A. W. Hyatt, C. F. Driscoll, and J. H. Malmberg, *Phys. Rev. Lett.* **59**, 2975 (1987).
 - [5] C. F. Driscoll and J. H. Malmberg, *Phys. Rev. Lett.* **50**, 167 (1983); see also C. F. Driscoll, K. S. Fine, and J. H. Malmberg, *Phys. Fluids* **29**, 2015 (1986).
 - [6] G. Gabrielse *et al.*, *Phys. Rev. Lett.* **65**, 1317 (1990); R. S. Van Dyck, Jr., F. L. Moore, D. L. Farnham, and P. B. Schwinberg, *Phys. Rev. A* **40**, 6308 (1989).
 - [7] D. H. E. Dubin, *Phys. Rev. Lett.* **66**, 2076 (1991).
 - [8] R. C. Davidson, *Physics of Nonneutral Plasmas* (Addison-Wesley, Redwood City, 1990).
 - [9] S. A. Prasad and T. M. O'Neil, *Phys. Fluids* **26**, 665 (1983); see also **27**, 206 (1984).
 - [10] J. S. DeGrassie and J. H. Malmberg, *Phys. Fluids* **23**, 63 (1980).
 - [11] R. H. Levy, *Phys. Fluids* **11**, 920 (1968).
 - [12] Roy W. Gould (to be published).
 - [13] S. A. Prasad, G. J. Morales, and B. D. Fried, *Phys. Fluids* **30**, 3093 (1987).
 - [14] I. B. Bernstein, *Phys. Rev.* **109**, 10 (1958).
 - [15] S. J. Buchsbaum and A. Hasegawa, *Phys. Rev. Lett.* **12**, 685 (1964); *Phys. Rev.* **143**, 303 (1966).
 - [16] G. A. Pearson, *Phys. Fluids* **9**, 2464 (1966).